Available online at www.sciencedirect.com
ScienceDirect
Journal of Computational Physics 227 (2007) 1411–1427
JOURNAL OF COMPUTATIONAL PHYSICS
www.elsevier.com/locate/jcp

An energy law preserving C^0 finite element scheme for simulating the kinematic effects in liquid crystal dynamics

Ping Lin [a,*], Chun Liu [b], Hui Zhang [c]

[a] Department of Mathematics, The National University of Singapore, Singapore 117543, Singapore
[b] Department of Mathematics, Pennsylvania State University, University Park, PA 18601, USA
[c] School of Mathematical Sciences, Beijing Normal University, Beijing 100875, PR China

Received 8 January 2007; received in revised form 2 August 2007; accepted 6 September 2007
Available online 18 September 2007

Abstract

In this paper, we use finite element methods to simulate the hydrodynamical systems governing the motions of nematic liquid crystals in a bounded domain Ω. We reformulate the original model in the weak form which is consistent with the continuous dissipative energy law for the flow and director fields in $\mathbf{W}^{1,2+\sigma}(\Omega)$ ($\sigma > 0$ is an arbitrarily small number). This enables us to use convenient conformal C^0 finite elements in solving the problem. Moreover, a discrete energy law is derived for a modified midpoint time discretization scheme. A fixed iterative method is used to solve the resulted nonlinear system so that a matrix free time evolution may be achieved and velocity and director variables may be solved separately. A number of hydrodynamical liquid crystal examples are computed to demonstrate the effects of the parameters and the performance of the method.

MSC: 65M60; 76A15

Keywords: Liquid crystal flow; Non-Newtonian fluids; C^0 finite element approximation; Discrete energy law; Singularity dynamics

1. Introduction

The hydrodynamical and rheological properties of liquid crystals materials are determined by the competition between the kinetic enery and the internal elastic energies. The latter is represented in terms of the orientational order parameter **d**, represents the alignment of the polar molecules of the materials. In the meantime, the special coupling between the kinematic transport of the molecules and the induced elastic stresses that affect the flow field give many interesting and complicated hydrodynamical phenomena that is specially dependent on the materials.

* Corresponding author. Tel.: +65 65162488; fax: +65 67795452.
E-mail addresses: matlinp@math.nus.edu.sg (P. Lin), liu@math.psu.edu (C. Liu), hzhang@bnu.edu.cn (H. Zhang).

0021-9991/$ - see front matter
doi:10.1016/j.jcp.2007.09.005

For the macroscopic continuum description of the hydrodyanamics of the nematic liquid crystals, Ericksen and Leslie derived the following nonlinear coupled system [5,7,16] for those materials with isotropic elastic energies:

$$\mathbf{u}_t + (\mathbf{u}\cdot\nabla)\mathbf{u} - \nu\nabla\cdot D(\mathbf{u}) + \nabla p - \lambda\nabla\cdot((\nabla\mathbf{d})^{\mathrm{T}}\nabla\mathbf{d}) - \lambda\nabla\cdot(\beta(\Delta\mathbf{d}-\mathbf{f}(\mathbf{d}))\mathbf{d}^{\mathrm{T}} + (\beta+1)\mathbf{d}(\Delta\mathbf{d}-\mathbf{f}(\mathbf{d}))^{\mathrm{T}}) = 0, \tag{1.1}$$

$$\nabla\cdot\mathbf{u} = 0, \tag{1.2}$$

$$\mathbf{d}_t + (\mathbf{u}\cdot\nabla)\mathbf{d} + \beta(\nabla\mathbf{u})\mathbf{d} + (\beta+1)(\nabla\mathbf{u})^{\mathrm{T}}\mathbf{d} - \gamma(\Delta\mathbf{d}-\mathbf{f}(\mathbf{d})) = 0 \tag{1.3}$$

with initial and boundary conditions

$$\mathbf{u}|_{t=0} = \mathbf{u}_0, \quad \mathbf{d}|_{t=0} = \mathbf{d}_0, \quad \mathbf{u}|_{\partial\Omega} = \mathbf{u}_0|_{\partial\Omega} = \mathbf{g}_{\mathbf{u}}, \quad \mathbf{d}|_{\partial\Omega} = \mathbf{d}_0|_{\partial\Omega} = \mathbf{g}_{\mathbf{d}}. \tag{1.4}$$

Here $\mathbf{u}$ represents the velocity of the liquid crystal flow, p the pressure, and $\mathbf{d}$ the orientation of the liquid crystal molecules, $\mathbf{u},\mathbf{d}:\Omega\times\mathbb{R}^+\to\mathbb{R}^n$, $p:\Omega\times\mathbb{R}^+\to\mathbb{R}$ and $\Omega\subset\mathbb{R}^n$. $\beta\in[-1,0]$ is a constant and μ, λ and γ are positive constants. In this paper we will only consider $n=2$, i.e. two dimensional cases. But the method applies to three dimensional cases. We define the strain rate $D(\mathbf{u}) = (1/2)(\nabla\mathbf{u} + (\nabla\mathbf{u})^{\mathrm{T}})$, the gradients of the director field take the standard notation as:

$$(\nabla\mathbf{d})_{ij} = \mathbf{d}_{i,j} = \frac{\partial d_i}{\partial x_j}$$

and $\mathbf{f}(\mathbf{d}) = (1/\epsilon^2)(|\mathbf{d}|^2-1)\mathbf{d}$ may be seen as a penalty function to approximate the constraint $|\mathbf{d}|=1$ which is due to liquid crystal molecules being of similar size. This penalty term is also physically meaningful and represents a possible relaxation of molecules from the strict unit-length constraint. The function $\mathbf{f}(\mathbf{d})$ is the gradient of the scalar valued function $F(\mathbf{d}) = (1/4\epsilon^2)(|\mathbf{d}|^2-1)^2$. The divergence operator of a matrix is defined as

$$(\nabla\cdot A)_i = a_{ij,j} = \sum_j \frac{\partial a_{ij}}{\partial x_j}.$$

For convenience of writing later we define

$$D_\beta(\mathbf{u}) = \beta\nabla\mathbf{u} + (\beta+1)(\nabla\mathbf{u})^{\mathrm{T}} \tag{1.5}$$

The first equation in the system is the equation for the conservation of linear momentum (the force balance equation). It combines a usual equation describing the flow of an isotropic fluid and an extra nonlinear coupling term which is anisotropic. This extra term is the induced elastic stress from the elastic energy through the transport in the third equation. The second equation represents incompressibility of the liquid. The third equation is associated with conservation of the angular momentum. We want to point out the transport of the director, $\mathbf{d}_t + (\mathbf{u}\cdot\nabla)\mathbf{d} + D_\beta(\mathbf{u})\mathbf{d}$, reflects the microscopic picture of those ellipsoid shaped molecules moving in Stokes fluids with no slip boundary conditions on the particle surfaces [11,12]. It presents an effective stretching effect on the director $\mathbf{d}$. For this, we are going to give some brief explanations:

Due to the fact that $\mathbf{d}$ being a vector, we have to take into account of its tendency of response to the stretching in the flow field. For this, we will look at the deformation tensor F associated with the flow field,

$$F_{ij} = \frac{\partial x_i}{\partial X_j}.$$

The simple chain rule gives the following transport property of F [24,17]

$$F_t + (\mathbf{u}\cdot\nabla)F = (\nabla\mathbf{u})F, F_t^{-\mathrm{T}} + (\mathbf{u}\cdot\nabla)F^{-\mathrm{T}} = -(\nabla\mathbf{u})^{\mathrm{T}}F^{-\mathrm{T}}.$$

Suppose the liquid crystal molecule is of rod-like shape, with infinite aspect ratio, the transport of the direction of the rod $\mathbf{d}$ can be expressed as

$$\mathbf{d}(x(X,t),t) = F\mathbf{d}_0(X),$$

which clearly demonstrates the stretching of the director besides the transport along the trajectory. Moreover, taking the derivative with respect to t gives

$$\mathbf{d}_t + (\mathbf{u}\cdot\nabla)\mathbf{d} = F_t\mathbf{d}_0 + (\mathbf{u}\cdot\nabla)F\mathbf{d}_0 = (\nabla\mathbf{u})F\mathbf{d}_0 = (\nabla\mathbf{u})\mathbf{d}.$$

Hence the total derivative of the director here is

$$\frac{D}{Dt}\mathbf{d} = \mathbf{d}_t + (\mathbf{u}\cdot\nabla)\mathbf{d} - (\nabla\mathbf{u})\mathbf{d}.$$

In general, for a molecule of ellipsoid shape with a finite aspect ratio, the transport of the main axis direction can be represented by

$$\mathbf{d}(x(X,t),t) = E\mathbf{d}_0(X),$$

where E is the infinitesimal generators of F and $F^{-\mathrm{T}}$ that were in the linear combination and satisfies the following transport equation:

$$E_t + (\mathbf{u}\cdot\nabla)E = -(\beta\nabla\mathbf{u} + (1+\beta)(\nabla\mathbf{u})^{\mathrm{T}})E.$$

From this point of view we say that $D_\beta(\mathbf{u})$ has an effective stretching effect from the shape of molecules. This will give the transport like:

$$\frac{D}{Dt}\mathbf{d} = \mathbf{d}_t + (\mathbf{u}\cdot\nabla)\mathbf{d} + \beta(\nabla\mathbf{u})\mathbf{d} + (1+\beta)(\nabla\mathbf{u})^{\mathrm{T}}\mathbf{d} = \mathbf{d}_t + (\mathbf{u}\cdot\nabla)\mathbf{d} - \omega(\mathbf{u})\mathbf{d} + (2\beta+1)D(\mathbf{u})\mathbf{d}.$$

Again here we use the notation $\omega(\mathbf{u})$ being the skew-symmetric part of $\nabla\mathbf{u}$ and $D(\mathbf{u})$ the symmetric part [5,7].

It is obvious to see that, when $\beta = -0.5$, the molecules take the spherical shape and the transport by the flow field reduces to the transport of the flow and the rigid rotation.

It is a remarkable property that the system (1.1)–(1.3) possesses exactly the same energy dissipative law, independent to the kinematic transport $\mathbf{d}_t + (\mathbf{u}\cdot\nabla)\mathbf{d} + D_\beta(\mathbf{u})\mathbf{d}$:

$$\frac{\mathrm{d}E}{\mathrm{d}t} = -(\nu\|D(\mathbf{u})\|^2_{L^2(\Omega)} + \lambda\gamma\|\Delta\mathbf{d} - \mathbf{f}(\mathbf{d})\|^2_{L^2(\Omega)}), \tag{1.6}$$

where

$$E = \frac{1}{2}\|\mathbf{u}\|^2_{L^2(\Omega)} + \frac{\lambda}{2}\|\nabla\mathbf{d}\|^2_{L^2(\Omega)} + \lambda\int_\Omega F(\mathbf{d}).$$

The analytical results in [15,16] indicated that these energy laws are particularly important when the singularities are involved in our study of hydrodynamical motions of these liquid crystal materials. The physical singularities we are seeking/tracking are those energetically admissible ones. Hence the naive numerical schemes which may not preserve the energy equalities can result in the loss of the accuracy of the numerical scheme and the presence of artificial singularities.

There have been several previous attempts in this direction, especially in the case of small molecules situations, where the effect of the molecular stretching/rotation (or the term $D_\beta(\mathbf{u})$) is ignored. Notice in deriving this energy law (1.6) the test function $-(\Delta\mathbf{d} - \mathbf{f}(\mathbf{d}))$ is used (implying that the test function space should be in $\mathbf{H}^2$) a C^1 (or $\mathbf{H}^2$ conforming) finite element method is adopted in [21] to solve the system (1.1)–(1.3) in order to keep the energy law after the spatial discretization. But the construction and implementation of C^1 elements are complicated. In [23] a mixed finite element method is applied to the system to avoid the C^1 element. But the introduction of the new variable $\nabla\mathbf{d}$ increases quite a few number of unknown variables and complication of implementation. A spectral method is also studied in [3]. Recently in [20] a direct weak formulation is introduced and a C^0 finite element method may be used with this formulation. The following reformulated energy law associated with this formulation is only formally derived there.

$$\frac{\mathrm{d}}{\mathrm{d}t}\left(\frac{1}{2}\|\mathbf{u}\|^2_{L^2} + \frac{\lambda}{2}\|\nabla\mathbf{d}\|^2_{L^2} + \lambda\int_\Omega F(\mathbf{d})\right) = -\left(\nu\|\nabla\mathbf{u}\|^2_{L^2} + \frac{\lambda}{\gamma}\|\mathbf{d}_t + (\mathbf{u}\cdot\nabla)\mathbf{d}\|^2_{L^2}\right). \tag{1.7}$$

We can see if the solution is so regular that the director equation holds then these two energy laws are the same. The latter energy law allows lower regularity of the solution. But it is not derived rigorously based on the weak form where the C^0 finite element method is used, although the discrete energy decay is verified through a number of numerical experiments in [20]. In fact, based on this direct weak formulation the energy law (1.7) is not valid in general in a C^0 finite element space.

One different issue of the system (1.1)–(1.3) from the small molecule system (when $D_\beta(\mathbf{u})\mathbf{d}$ term is absent from the transport equation) is that, the maximal principle holds in the latter case and not the former one. This brings extra difficulties in the analytical study of the system. However, in all the numerical examples we computed in this paper it seems that the director does not get stretched beyond the unit length. We also notice the recent work in [25], which demonstrate the dramatic effects of the transport to the overall dynamics of the flow, in that case, the annihilation speed of the point defects in the axial-symmetric geometries.

In the small molecule model $\Delta\mathbf{d}$ does not explicitly appear in the flow equation so we can directly obtain a weak form which requires only $\mathbf{W}^{1,2+\sigma}$ regularity in 2D (or $W^{1,3}$ in 3D) for $\mathbf{u}$ and $\mathbf{d}$, where σ can be an arbitrarily small positive number. Thus the C^0 (conforming) finite element method may be used directly (although not enough for a rigorous energy law). In the current transport case $\Delta\mathbf{d}$ appears explicitly. Its direct weak form requires $\mathbf{H}^2$ regularity and usually C^1 finite elements are required in order to maintain the energy law. In this paper we will first reformulate the flow equation using the director field equation to express $\Delta\mathbf{d}$ and obtaining a flow equation without $\Delta\mathbf{d}$. Then we write down its weak form where only $W^{1,2+\sigma}$ regularity is required for $\mathbf{d}$ and $\mathbf{u}$. We can then apply the Galerkin finite element method with C^0 finite elements to the reformulated system. The benefits of using C^0 elements over C^1 elements are obvious. The method can be implemented easily and many existing codes and mesh generators may be incorporated to reduce computational complication. Unlike [20] the energy law can be justified rigorously with this weak form and with the corresponding C^0 finite element method. The reformulation and energy law will be given in Section 2. Furthermore, in Section 3 we present a temporal second order C^0 finite element scheme. It is a modified midpoint scheme and a discrete energy law is derived for this scheme. To our knowledge, such a fully discrete energy law has never been done before in fluid flow computations. We also remark that a method preserving the energy law of the model should be more reliable than a method without it, especially in this liquid crystal flow case since the energy law is the key to produce correct dynamics. In Section 4 we present an efficient way to solve the resulted nonlinear system by a fixed point iteration which formulates a matrix free time evolution. Moreover, with this iterative method the flow field and director field are automatically separated. We can thus solve the discrete system more efficiently since a direct linear system solver for the flow equations or the director equation is only needed at the initial time but is not needed at later time steps. We will use the method to simulate a few liquid crystal flow examples with various parameters and domain geometries and will recognize difference to small molecule cases in Section 5. We will also show a case (Fig. 5) where the energy law preserving scheme performs better than the method given in [20]. We hope that these computational results would motivate further theoretical study of the model. Other computational results for microstructure of 2D and 3D liquid crystal materials (without the flow field) may be found in [9,1,8,22] and references therein.

2. Weak formulation and continuous energy law

Let Ω be a bounded domain of $\mathbb{R}^2$. We denote by Γ the boundary of Ω, and we suppose that Γ is sufficiently smooth (for example, Lipschitz-continuous). Define the spaces $\mathbf{W}^{1,2+\sigma}(\Omega) = (W^{1,2+\sigma}(\Omega))^2$, $\mathbf{W}_{\mathbf{g}}^{1,2+\sigma} = \{\mathbf{u} \in \mathbf{W}^{1,2+\sigma}(\Omega), \mathbf{u} = \mathbf{g} \text{ on } \Gamma\}$, $\mathbf{L}^2(\Omega) = (L^2(\Omega))^2$ and $L_0^2(\Omega) = \{p \in L^2(\Omega), \int_\Omega p\,\mathrm{d}\mathbf{x} = 0\}$, where $\sigma > 0$ can be arbitrarily small.

From the director Eq. (1.3) we can express

$$\Delta\mathbf{d} = \frac{1}{\gamma}\big(\mathbf{d}_t + (u\cdot\nabla)\mathbf{d} + (D_\beta\mathbf{u})\mathbf{d} + \gamma\mathbf{f}(\mathbf{d})\big).$$

We then have (cf. [23,20])

$$\begin{aligned}\nabla\cdot\Big((\nabla\mathbf{d})^{\mathrm{T}}\nabla\mathbf{d}\Big) &= (\nabla\mathbf{d})^{\mathrm{T}}\Delta\mathbf{d} + \nabla(|\nabla\mathbf{d}|^2)/2\\ &= \frac{1}{\gamma}(\nabla\mathbf{d})^{\mathrm{T}}\big(\mathbf{d}_t + (\mathbf{u}\cdot\nabla)\mathbf{d} + D_\beta(\mathbf{u})\mathbf{d}\big) + \nabla\Big(|\nabla\mathbf{d}|^2/2 + F(\mathbf{d})\Big),\end{aligned} \tag{2.1}$$

$$\nabla\cdot\big((\Delta\mathbf{d} - \mathbf{f}(\mathbf{d}))\mathbf{d}^{\mathrm{T}}\big) = \frac{1}{\gamma}\nabla\cdot\big((\mathbf{d}_t + (\mathbf{u}\cdot\nabla)\mathbf{d} + D_\beta(\mathbf{u})\mathbf{d})\mathbf{d}^{\mathrm{T}}\big)$$

and

$$\nabla\cdot\Big(\mathbf{d}(\Delta\mathbf{d}-\mathbf{f}(\mathbf{d}))^{\mathrm{T}}\Big)=\frac{1}{\gamma}\nabla\cdot\Big(\mathbf{d}(\mathbf{d}_t+(\mathbf{u}\cdot\nabla)\mathbf{d}+D_\beta(\mathbf{u})\mathbf{d})^{\mathrm{T}}\Big),$$

where $D_\beta(\mathbf{u})$ is defined in (1.5). Substituting above relations to the flow Eq. (1.1) and defining a new pressure $p:=p+|\nabla\mathbf{d}|^2/2$ result in an equation without $\Delta\mathbf{d}$. By multiplying $\mathbf{v}$ and $\mathbf{e}$ to the first and the third equations, respectively, We can obtain the following weak form:

Find $\mathbf{u}\in\mathbf{W}^{1,2+\sigma}_{\mathbf{g_u}}(\Omega)$, $p\in L^2_0(\Omega)$ and $\mathbf{d}\in\mathbf{W}^{1,2+\sigma}_{\mathbf{g_d}}(\Omega)$ such that

$$\int_\Omega\Big(\mathbf{u}_t\cdot\mathbf{v}+(\mathbf{u}\cdot\nabla)\mathbf{u}\cdot\mathbf{v}+\nu\nabla\mathbf{u}:\nabla\mathbf{v}-p(\nabla\cdot\mathbf{v})+\frac{\lambda}{\gamma}\big(\mathbf{d}_t+(\mathbf{u}\cdot\nabla)\mathbf{d}+D_\beta(\mathbf{u})\mathbf{d}\big)\cdot(\mathbf{v}\cdot\nabla)\mathbf{d}$$
$$+\frac{\lambda}{\gamma}\big(\mathbf{d}_t+(\mathbf{u}\cdot\nabla)\mathbf{d}+D_\beta(\mathbf{u})\mathbf{d}\big)\cdot D_\beta(\mathbf{v})\mathbf{d}\Big)\,\mathrm{d}\mathbf{x}=0,\quad\forall\mathbf{v}\in\mathbf{W}^{1,2+\sigma}_0(\Omega),\tag{2.2}$$

$$\int_\Omega(\nabla\cdot\mathbf{u})q\,\mathrm{d}\mathbf{x}=0,\quad\forall q\in L^2(\Omega),\tag{2.3}$$

$$\int_\Omega\big(\mathbf{d}_t\cdot\mathbf{e}+(\mathbf{u}\cdot\nabla)\mathbf{d}\cdot\mathbf{e}+D_\beta(\mathbf{u})\mathbf{d}\cdot\mathbf{e}+\gamma(\nabla\mathbf{d}:\nabla\mathbf{e}+\mathbf{f}(\mathbf{d})\cdot\mathbf{e})\big)\,\mathrm{d}\mathbf{x}=0,\quad\forall\mathbf{e}\in\mathbf{W}^{1,2+\sigma}_0,\tag{2.4}$$

where ":" represents an inner product of two matrices, i.e. $A:B=\sum_i\sum_j a_{ij}b_{ij}$ (also denoting $|A|^2=A:A$) and we have used the facts that

$$(\nabla\mathbf{d})^{\mathrm{T}}\mathbf{w}\cdot\mathbf{v}=\mathbf{w}\cdot(\mathbf{v}\cdot\nabla)\mathbf{d}\quad\text{and}\quad\mathbf{w}\mathbf{d}^{\mathrm{T}}:\nabla\mathbf{v}=\mathbf{w}\cdot(\nabla\mathbf{v})\mathbf{d}=\mathbf{d}\cdot(\nabla\mathbf{v})^{\mathrm{T}}\mathbf{w}.\tag{2.5}$$

More precisely, the pressure p should be in space $L_0^{\frac{2+\sigma}{1+\sigma}}$. For simplicity of writing, we just use a little bit smaller space L^2_0. It does not matter when we apply the finite element approximate space later.

With this weak form the energy law can be readily obtained when $\mathbf{u}$ and $\mathbf{d}$ satisfy homogeneous boundary conditions. Taking $\mathbf{v}=\mathbf{u}$ and $\mathbf{e}=(\lambda/\gamma)\mathbf{d}_t$ in (2.2) and (2.4), respectively, summing them up and using integral identities (where (2.3) is used)

$$\int_\Omega(\mathbf{u}\cdot\nabla)\mathbf{u}\cdot\mathbf{u}\,\mathrm{d}\mathbf{x}=\frac{1}{2}\int_\Omega\mathbf{u}\cdot\nabla|\mathbf{u}|^2=0,\tag{2.6}$$

we have the following energy law:

$$\frac{\mathrm{d}}{\mathrm{d}t}\left(\frac{1}{2}\|\mathbf{u}\|^2_{L^2}+\frac{\lambda}{2}\|\nabla\mathbf{d}\|^2_{L^2}+\lambda\int_\Omega F(\mathbf{d})\right)=-\left(\nu\|\nabla\mathbf{u}\|^2_{L^2}+\frac{\lambda}{\gamma}\|\mathbf{d}_t+(\mathbf{u}\cdot\nabla)\mathbf{d}+D_\beta(\mathbf{u})\mathbf{d}\|^2_{L^2}\right).\tag{2.7}$$

This indicates that the energy decays with time. A discrete energy law can be similarly obtained with a modified convection in (2.2) (see the following section) and is the same as (2.7) if C^0 finite elements are used and if the time remains continuous as long as such finite element solution belongs to the functional spaces required in (2.2)–(2.4). We will give a discrete energy law for a fully discretized system in the following section.

3. A modified midpoint scheme with C^0 finite elements and discrete energy law

Solutions of the weak problem (2.2)–(2.4) are approximated using a finite difference scheme in time and a finite element method in space. Due to solution singularities associated to this type of problems maintaining its energy law may be important to do a good simulation job. Such a law is also important to serve as a justification in simulation of complex systems involving complex fluids equations since almost no benchmark solution is available. In existing numerical methods (cf. [23] and references therein) the discrete energy law can only be derived for the semi-discrete case where the time remains continuous. Such a derivation is usually a trivial application of the argument for the continuous energy law as long as the finite element space is conformal to the space where the solution locates. In [20] even such a semi-discrete energy law cannot be made rigorous. Since in the weak form derived earlier we only require the solution in space $\mathbf{W}^{1,2+\sigma}$ ($\sigma>0$) we can then use conformal C^0 finite element for the spatial discretization without any problem. In

the temporal direction, since the liquid crystal flow model is highly nonlinear, explicit–implicit (or semi-implicit) first order schemes are usually adopted (cf. [20]), where one part of the nonlinear term is treated explicitly and the other part is treated implicitly. The fully implicit backward Euler scheme is also used frequently in computational fluid dynamics. Later in this section we will remark about a possible approximate discrete energy law for these two first order schemes. Nevertheless, our major goal in this section is to present a second order temporal scheme which turns out to have an accurate discrete energy law. The nonlinear system resulted from the discretization should be solved by a fast and efficient method, which will be discussed in the following section.

Let

$$\mathcal{W} = \mathbf{W}_{\mathbf{g_u}}^{1,2+\sigma}(\Omega) \times L_0^2(\Omega) \times \mathbf{W}_{\mathbf{g_d}}^{1,2+\sigma}(\Omega)$$

and $\mathcal{W}^h = \mathcal{U}^h \times \mathcal{P}^h \times \mathcal{H}^h \subset \mathcal{W}$ be a finite dimensional subspace of $\mathcal{W}$ given by a finite element discretization of Ω. $\mathcal{W}_0^h$ represents the space $\mathcal{W}^h$ satisfying homogeneous Dirichlet boundary conditions. If $\Delta t > 0$ represents a time step size and $(\mathbf{u}_h^n, p_h^n, \mathbf{d}_h^n) \in \mathcal{W}^h$ is an approximation of $\mathbf{u}(t^n) = \mathbf{u}(n\Delta t)$, $p(t^n) = p(n\Delta t)$ and $\mathbf{d}(t^n) = \mathbf{d}(n\Delta t)$, the approximation at time $t^{n+1} = (n+1)\Delta t$ is computed as the solution of $(\mathbf{u}_h^{n+1}, p_h^{n+1}, \mathbf{d}_h^{n+1}) \in \mathcal{W}^h$ by the following scheme

$$\begin{aligned}
&\int_\Omega \Bigg(\mathbf{u}_t^{n+1} \cdot \mathbf{v} + (\mathbf{u}_h^{n+\frac{1}{2}} \cdot \nabla)\mathbf{u}_h^{n+\frac{1}{2}} \cdot \mathbf{v} + \frac{1}{2}(\nabla \cdot \mathbf{u}_h^{n+\frac{1}{2}})\mathbf{u}_h^{n+\frac{1}{2}} \cdot \mathbf{v} + \nu \nabla \mathbf{u}_h^{n+\frac{1}{2}} : \nabla \mathbf{v} - p_h^{n+\frac{1}{2}}(\nabla \cdot \mathbf{v}) \\
&\quad + \frac{\lambda}{\gamma}\left(\mathbf{d}_t^{n+1} + (\mathbf{u}_h^{n+\frac{1}{2}} \cdot \nabla)\mathbf{d}_h^{n+\frac{1}{2}} + D_\beta(\mathbf{u}_h^{n+\frac{1}{2}})\mathbf{d}_h^{n+\frac{1}{2}} \right) \cdot (\mathbf{v} \cdot \nabla)\mathbf{d}_h^{n+\frac{1}{2}} \\
&\quad + \frac{\lambda}{\gamma}\left(\mathbf{d}_t^{n+1} + (\mathbf{u}_h^{n+\frac{1}{2}} \cdot \nabla)\mathbf{d}_h^{n+\frac{1}{2}} + D_\beta(\mathbf{u}_h^{n+\frac{1}{2}})\mathbf{d}_h^{n+\frac{1}{2}} \right) \cdot D_\beta(\mathbf{v})\mathbf{d}_h^{n+\frac{1}{2}} \Bigg) \mathrm{d}\mathbf{x} = 0,
\end{aligned} \tag{3.1}$$

$$\int_\Omega (\nabla \cdot \mathbf{u}_h^{n+\frac{1}{2}}) q \, \mathrm{d}\mathbf{x} = 0, \tag{3.2}$$

$$\int_\Omega \left(\mathbf{d}_t^{n+1} \cdot \mathbf{e} + (\mathbf{u}_h^{n+\frac{1}{2}} \cdot \nabla)\mathbf{d}_h^{n+\frac{1}{2}} \cdot \mathbf{e} + D_\beta(\mathbf{u}^{n+\frac{1}{2}})\mathbf{d}_h^{n+\frac{1}{2}} \cdot \mathbf{e} + \gamma \nabla \mathbf{d}_h^{n+\frac{1}{2}} : \nabla \mathbf{e} + \frac{\gamma}{\epsilon^2}\mathbf{g}_h(\mathbf{d}_h^n, \mathbf{d}_h^{n+1}) \cdot \mathbf{e} \right) \mathrm{d}\mathbf{x} = 0, \tag{3.3}$$

for all $(\mathbf{v}, q, \mathbf{e}) \in \mathcal{W}_0^h$, where $\mathbf{u}_t^{n+1} = \frac{\mathbf{u}_h^{n+1} - \mathbf{u}_h^n}{\Delta t}$, $\mathbf{d}_t^{n+1} = \frac{\mathbf{d}_h^{n+1} - \mathbf{d}_h^n}{\Delta t}$, $\mathbf{u}_h^{n+\frac{1}{2}} = \frac{1}{2}(\mathbf{u}_h^n + \mathbf{u}_h^{n+1})$, $\mathbf{d}_h^{n+\frac{1}{2}} = \frac{1}{2}(\mathbf{d}_h^n + \mathbf{d}_h^{n+1})$, $p_h^{n+\frac{1}{2}} = \frac{1}{2}(p_h^n + p_h^{n+1})$, and

$$\mathbf{g}_h(\mathbf{d}_h^n, \mathbf{d}_h^{n+1}) = \frac{(|\mathbf{d}_h^{n+1}|^2 - 1) + (|\mathbf{d}_h^n|^2 - 1)}{2} \frac{\mathbf{d}_h^{n+1} + \mathbf{d}_h^n}{2} \tag{3.4}$$

is an approximation to the nonlinear function $\mathbf{g}(\mathbf{d}) = (|\mathbf{d}|^2 - 1)\mathbf{d}$ in the director equation. It comes from a relaxation force due to the unit length constraint of liquid crystal molecules. Note that the extra term $\frac{1}{2}(\nabla \cdot \mathbf{u}_h^{n+\frac{1}{2}})\mathbf{u}_h^{n+\frac{1}{2}}$ added in (3.1) corresponds to adding a zero term $\frac{1}{2}(\nabla \cdot \mathbf{u})\mathbf{u}$ to (1.1) following the technique mentioned in [26] in studying the pseudo-compressibility method. The reason we add this term here is a technical need in deriving a discrete energy law for this scheme and for the penalized scheme later. In existing work on liquid crystal flows continuous energy law is usually considered. The situation may be different in the discrete case. Unlike the integral identity (2.6) the divergence free Eq. (3.2) does not eliminate the convection term $(\mathbf{u}_h^{n+\frac{1}{2}} \cdot \nabla)\mathbf{u}_h^{n+\frac{1}{2}} \cdot \mathbf{v}$ (since $|\mathbf{u}_h^{n+\frac{1}{2}}|^2$ may not necessarily be in the finite element space of q) when taking $\mathbf{v} = \mathbf{u}_h^{n+\frac{1}{2}}$ later in deriving a discrete energy law.

If there were no unit length relaxation term $\mathbf{g}_h$ the scheme given above would be just the midpoint scheme. The approximation $\mathbf{g}_h$ looks similar to the midpoint scheme but not exactly the same. We may call it a modified midpoint scheme. The approximate unit length relaxation term $\mathbf{g}_h$ is so designed that we are able to derive an accurate discrete energy law for the fully discrete system. The resulting system of the scheme may be solved by a Newton or fixed point iterative method. We will discuss it in the following section.

Now we derive the discrete energy law assuming the homogeneous boundary condition for $\mathbf{u}$ and the time-independent boundary condition for $\mathbf{d}$. For a nonhomogeneous boundary condition one can usually change it to the homogeneous boundary condition through a variable transformation. According to the continuous case, we take $\mathbf{v} = \mathbf{u}_h^{n+\frac{1}{2}}$ and $\mathbf{e} = \frac{\lambda}{\gamma}\mathbf{d}_t^{n+1}$. We can readily have

$$\int_\Omega \left[(\mathbf{u}_h^{n+\frac{1}{2}} \cdot \nabla)\mathbf{u}_h^{n+\frac{1}{2}} \cdot \mathbf{u}_h^{n+\frac{1}{2}} + \frac{1}{2}(\nabla \cdot \mathbf{u}_h^{n+\frac{1}{2}})\mathbf{u}_h^{n+\frac{1}{2}} \cdot \mathbf{u}_h^{n+\frac{1}{2}} \right] = 0 \tag{3.5}$$

since $\mathbf{u}_h^{n+\frac{1}{2}}$ is zero at the boundary,

$$\mathbf{u}_{\bar{t}}^{n+1} \cdot \mathbf{u}_h^{n+\frac{1}{2}} = \frac{1}{2}\frac{\mathbf{u}_h^{n+1} \cdot \mathbf{u}_h^{n+1} - \mathbf{u}_h^n \cdot \mathbf{u}_h^n}{\Delta t} = \frac{1}{2}(|\mathbf{u}_h^{n+1}|^2)_{\bar{t}} \tag{3.6}$$

and

$$\nabla \mathbf{d}_h^{n+\frac{1}{2}} : \nabla \mathbf{d}_{\bar{t}}^{n+1} = \nabla d_1^{n+\frac{1}{2}} \cdot \nabla (d_1)_{\bar{t}}^{n+1} + \nabla d_2^{n+\frac{1}{2}} \cdot \nabla (d_2)_{\bar{t}}^{n+1} = \frac{1}{2}(|\nabla d_1^{n+1}|^2)_{\bar{t}} + \frac{1}{2}(|\nabla d_2^{n+1}|^2)_{\bar{t}} = \frac{1}{2}(|\nabla \mathbf{d}_h^{n+1}|^2)_{\bar{t}}, \tag{3.7}$$

where $\mathbf{d}_h = (d_1, d_2)^{\mathrm{T}}$. We can also have

$$\begin{aligned} \mathbf{g}_h(\mathbf{d}_h^n, \mathbf{d}_h^{n+1}) \cdot \mathbf{d}_{\bar{t}}^{n+1} &= \frac{1}{4}(|\mathbf{d}_h^{n+1}|^2 + |\mathbf{d}_h^n|^2 - 2)(\mathbf{d}_h^{n+1} + \mathbf{d}_h^n) \cdot (\mathbf{d}_h^{n+1} - \mathbf{d}_h^n)/\Delta t \\ &= \frac{1}{4\Delta t}(|\mathbf{d}_h^{n+1}|^2 + |\mathbf{d}_h^n|^2 - 2)(|\mathbf{d}_h^{n+1}|^2 - |\mathbf{d}_h^n|^2) = (F(\mathbf{d}_h^{n+1}))_{\bar{t}}. \end{aligned} \tag{3.8}$$

With above choice of $\mathbf{v}$ and $\mathbf{e}$, using these finite difference identities and adding up (3.1) and (3.3) we can then obtain a discrete energy law:

$$\left(\frac{1}{2}\|\mathbf{u}_h^{n+1}\|_{\mathbf{L}^2}^2 + \frac{\lambda}{2}\|\nabla \mathbf{d}_h^{n+1}\|_{\mathbf{L}^2}^2 + \lambda \int_\Omega F(\mathbf{d}_h^{n+1}) \right)_{\bar{t}} = -\left(\nu \|\nabla \mathbf{u}_h^{n+\frac{1}{2}}\|_{\mathbf{L}^2}^2 + \frac{\lambda}{\gamma}\|\mathbf{d}_{\bar{t}}^{n+1} + (\mathbf{u}_h^{n+\frac{1}{2}} \cdot \nabla)\mathbf{d}_h^{n+\frac{1}{2}} + D_\beta(\mathbf{u}_h^{n+\frac{1}{2}})\mathbf{d}_h^{n+\frac{1}{2}}\|_{\mathbf{L}^2}^2 \right). \tag{3.9}$$

We can easily see that the discrete energy decays as well and the energy law (2.7) is accurately preserved by this modified midpoint scheme. We will briefly discuss possible energy laws for other commonly used schemes in a remark below and then see that it is not usually possible to achieve such an accurate energy law in a fully discrete system.

The divergence free condition (3.2) need be treated carefully in incompressible flow computations. The projection method is simple but may be difficult to impose an artificial boundary condition and to derive a discrete energy law. On the other hand, from the viewpoint of differential algebraic equations, the incompressible flow model is of index two because the pressure does not show up in the divergence Eq. (3.2). The problem is thus not well-posed and index reduction is needed before applying a differential equation solver (see [18]). The penalty method (cf. [26]) is a simple formulation for such purpose. It does not require any artificial boundary condition and general C^0 polynomial elements can be used without a need to check the inf-sup condition beforehand although the condition may be automatically satisfied via the formulation [19]. The penalty formulation works pretty well for the small molecule case (cf. [20]). We thus use the penalty formulation again for this model. More importantly, we are able to derive a discrete energy law based on this formulation. The penalty formulation under our modified midpoint scheme is to replace (3.2) by the following:

$$\int_\Omega (\nabla \cdot \mathbf{u}_h^{n+\frac{1}{2}} + \delta p_h^{n+\frac{1}{2}}) q \, \mathrm{d}\mathbf{x} = 0. \tag{3.10}$$

Practically, the divergence free condition may be enforced by choosing a relatively small δ. We will choose $\delta = 10^{-6}$ in our computations. When it is necessary to use a larger δ in order to improve the stability and accuracy a sequential regularization formulation (see [18]) may be used to replace the penalty formulation. The derivation of the energy law is not much different from the non-penalized formulation. Only the pressure term in (3.1) (i.e. $-p_h^{n+\frac{1}{2}} \nabla \cdot \mathbf{u}_h^{n+\frac{1}{2}}$) is relevant to the divergence equation. Now replacing (3.2) by (3.10) the pressure term becomes

$$-\int_\Omega p_h^{n+\frac{1}{2}} \nabla \cdot \mathbf{u}_h^{n+1} = \delta \int_\Omega (p_h^{n+\frac{1}{2}})^2.$$

So under the penalty formulation we can still obtain a discrete energy law:

$$\left(\frac{1}{2}\|\mathbf{u}_h^{n+1}\|_{\mathbf{L}^2}^2+\frac{\lambda}{2}\|\nabla\mathbf{d}_h^{n+1}\|_{\mathbf{L}^2}^2+\lambda\int_\Omega F(\mathbf{d}_h^{n+1})\right)_{\bar{t}}$$
$$=-\left(\nu\|\nabla\mathbf{u}_h^{n+1}\|_{\mathbf{L}^2}^2+\delta\|p_h^{n+\frac{1}{2}}\|_{L^2}^2+\frac{\lambda}{\gamma}\|\mathbf{d}_{\bar{t}}^{n+1}+(\mathbf{u}_h^{n+\frac{1}{2}}\cdot\nabla)\mathbf{d}_h^{n+\frac{1}{2}}+D_\beta(\mathbf{u}_h^{n+\frac{1}{2}})\mathbf{d}_h^{n+\frac{1}{2}}\|_{\mathbf{L}^2}^2\right). \tag{3.11}$$

So when δ is sufficiently small the continuous energy law is fully maintained under the fully discretized penalty formulation.

Remark 3.1. In all the existing work the fully implicit backward Euler scheme (cf. [21]) or some explicit–implicit scheme (cf. [20]) are often used. But the discrete energy law for these schemes are not usually studied. We only consider the backward Euler scheme in this remark (i.e. approximating $\mathbf{u}_t$ and $\mathbf{d}_t$ by the backward divided difference, and $\{\mathbf{u},p,\mathbf{d}\}$ in all other terms of (2.2)–(2.4) by $\{\mathbf{u}_h^{n+1},p_h^{n+1},\mathbf{d}_h^{n+1}\}$). The explicit–implicit scheme can be discussed similarly. Let us first look at the unit length relaxation term $\gamma\mathbf{g}(\mathbf{d})/\epsilon^2$, where $\mathbf{g}(\mathbf{d})$ is approximated by $g_h(\mathbf{d}_h^n,\mathbf{d}_h^{n+1})=(|\mathbf{d}_h^{n+1}|^2-1)\mathbf{d}_h^{n+1}$. In deriving the energy law for this scheme (i.e. choosing $\mathbf{e}=\frac{\lambda}{\gamma}\mathbf{d}_{\bar{t}}^{n+1}$) it becomes

$$\lambda\int_\Omega F(\mathbf{d}_h^{n+1})_{\bar{t}}+\mathrm{ER}_h^n,$$

where the extra error term $\mathrm{ER}_h^n=\frac{\lambda\Delta t}{4\epsilon^2}(2(|\mathbf{d}_h^{n+1}|^2-1)|\mathbf{d}_{\bar{t}}^{n+1}|^2+(|\mathbf{d}_h^{n+1}|^2-1)_{\bar{t}}^2)$. If $|\mathbf{d}_h^n|^2-1\approx 0$ and $(|\mathbf{d}_h^{n+1}|^2-1)_{\bar{t}}\approx 0$ then this error would possibly be small. Later from numerical computations we will see the length of the approximate director would not be close to one near the orientation singularities and thus the error may be of $O(\Delta t/\epsilon^2)$ which is large if Δt is not much smaller than ϵ^2. This might cause some loss of accuracy in the singularity evolution. We may approximate $\mathbf{g}(\mathbf{d})$ by (3.4) then the extra error ER_h^n is gone (see our argument for the modified midpoint scheme). We can then derive a discrete energy law for the penalized backward Euler discrete system by taking $\mathbf{v}=\mathbf{u}_h^{n+1}$ and $\mathbf{e}=\frac{\lambda}{\gamma}\mathbf{d}_{\bar{t}}^{n+1}$. We can have (cf. [13,18])

$$\mathbf{u}_{\bar{t}}^{n+1}\cdot\mathbf{u}_h^{n+1}=(\mathbf{u}_h^{n+1}\cdot\mathbf{u}_h^{n+1})_{\bar{t}}-\mathbf{u}_{\bar{t}}^{n+1}\cdot\mathbf{u}_h^n=(\mathbf{u}_h^{n+1}\cdot\mathbf{u}_h^{n+1})_{\bar{t}}+(\mathbf{u}_h^{n+1}-\mathbf{u}_h^n)\cdot(\mathbf{u}_h^{n+1}-\mathbf{u}_h^n)/\Delta t-\mathbf{u}_{\bar{t}}^{n+1}\cdot\mathbf{u}_h^{n+1}.$$

So

$$\mathbf{u}_{\bar{t}}^{n+1}\cdot\mathbf{u}_h^{n+1}=\frac{1}{2}(|\mathbf{u}_h^{n+1}|^2)_{\bar{t}}+\frac{\Delta t}{2}|\mathbf{u}_{\bar{t}}^{n+1}|^2. \tag{3.12}$$

Similarly,

$$\begin{aligned}\nabla\mathbf{d}_h^{n+1}:\nabla\mathbf{d}_{\bar{t}}^{n+1}&=\nabla d_1^{n+1}\cdot\nabla(d_1)_{\bar{t}}^{n+1}+\nabla d_2^{n+1}\cdot\nabla(d_2)_{\bar{t}}^{n+1}\\&=\frac{1}{2}(|\nabla d_1^{n+1}|^2)_{\bar{t}}+\frac{\Delta t}{2}|\nabla(d_1)_{\bar{t}}^{n+1}|^2+\frac{1}{2}(|\nabla d_2^{n+1}|^2)_{\bar{t}}+\frac{\Delta t}{2}|\nabla(d_2)_{\bar{t}}^{n+1}|^2\\&=\frac{1}{2}(|\nabla\mathbf{d}_h^{n+1}|^2)_{\bar{t}}+\frac{\Delta t}{2}|\nabla\mathbf{d}_{\bar{t}}^{n+1}|^2,\quad\text{where }\mathbf{d}_h=(d_1,d_2)^{\mathrm{T}}.\end{aligned} \tag{3.13}$$

We also have

$$\int_\Omega(\mathbf{u}_h^{n+1}\cdot\nabla)\mathbf{u}_h^{n+1}\cdot\mathbf{u}_h^{n+1}=\frac{1}{2}\delta\int_\Omega p_h^{n+1}|\mathbf{u}_h^{n+1}|^2,\quad-\int_\Omega p_h^{n+1}\nabla\cdot\mathbf{u}_h^{n+1}=\delta\int_\Omega(p_h^{n+1})^2.$$

We can then obtain a discrete energy law:

$$\left(\frac{1}{2}\|\mathbf{u}_h^{n+1}\|_{\mathbf{L}^2}^2+\frac{\lambda}{2}\|\nabla\mathbf{d}_h^{n+1}\|_{\mathbf{L}^2}^2+\lambda\int_\Omega F(\mathbf{d}_h^{n+1})\right)_{\bar{t}}$$
$$=-\left(\nu\|\nabla\mathbf{u}_h^{n+1}\|_{\mathbf{L}^2}^2+\frac{1}{2}\delta\int_\Omega p_h^{n+1}|\mathbf{u}_h^{n+1}|^2+\delta\|p_h^{n+1}\|_{L^2}^2+\frac{\lambda}{\gamma}\|\mathbf{d}_{\bar{t}}^{n+1}+(\mathbf{u}_h^{n+1}\cdot\nabla)\mathbf{d}_h^{n+1}+D_\beta(\mathbf{u}_h^{n+1})\mathbf{d}_h^{n+1}\|_{\mathbf{L}^2}^2\right.$$
$$\left.+\frac{\Delta t}{2}\|\mathbf{u}_{\bar{t}}^{n+1}\|_{\mathbf{L}^2}^2+\frac{\lambda\Delta t}{2}\|\nabla\mathbf{d}_{\bar{t}}^{n+1}\|_{\mathbf{L}^2}^2\right). \tag{3.14}$$

Using the Sobolev inequality $\|\mathbf{u}\|_{\mathbf{L}^4}^2 \leqslant \gamma_S^2 \|\mathbf{u}\|_{\mathbf{L}^2} \|\nabla \mathbf{u}\|_{\mathbf{L}^2}$ we have

$$\frac{\delta}{2} \int_\Omega p_h^{n+1} |\mathbf{u}_h^{n+1}|^2 \leqslant \frac{\delta}{2} \|p_h^{n+1}\|_{L^2} \|\mathbf{u}_h^{n+1}\|_{\mathbf{L}^4}^2 \leqslant \frac{\delta}{2} \|p_h^{n+1}\|_{L^2}^2 + \frac{\delta \gamma_S^2}{8} \|\mathbf{u}_h^{n+1}\|_{\mathbf{L}^2}^2 \|\nabla \mathbf{u}_h^{n+1}\|_{\mathbf{L}^2}.$$

If we choose δ sufficiently small such that $\frac{1}{8} \delta \gamma_S^2 \|\mathbf{u}_h^{n+1}\|_{\mathbf{L}^2}^2 < \nu$ (where γ_S is the constant of the Sobolev inequality) then the second term of the right hand side of the discrete energy law (3.14) can be controlled by the sum of the first and the third terms. Thus the energy always decays for the penalized backward Euler scheme as well.

From (3.14) we may also say that the backward Euler scheme approximately preserves the energy law as long as quantities $\int_\Omega p_h^n |\mathbf{u}_h^{n+1}|^2$, $\|p_h^{n+1}\|_{L^2}^2$, $\|\mathbf{u}_t^{n+1}\|_{\mathbf{L}^2}^2$ and $\|\nabla \mathbf{d}_t^{n+1}\|_{\mathbf{L}^2}^2$ are of moderate size. However, the first three quantities may be of moderate size but the last one could be very large. For example, we compute the Example 5.1 given in the last section with $\epsilon = 1.0, 0.5, 0.1$ and 0.05, and depict, say, $\|p_h^{n+\frac{1}{2}}\|_{L^2}$ and $\|\mathbf{d}_t^{n+1}\|_{\mathbf{L}^2}$ versus time in Fig. 1.

From the figure, it seems that $\max_n \|p_h^{n+\frac{1}{2}}\|_{L^2}$ is roughly of order $1/\epsilon$ and its magnitude is of moderate size. But $\max_n \|\nabla \mathbf{d}_t^{n+1}\|_{\mathbf{L}^2}$ is roughly of order $1/\epsilon^2$, especially, the magnitude of $\|\nabla \mathbf{d}_t^{n+1}\|_{\mathbf{L}^2}^2$ when $\epsilon = 0.05$ may be as large as 300^2 near $t = 0.26$ (the annihilation time when two singularities meet). So to achieve a good approximate energy law, we have to choose $\Delta t \ll \epsilon^2$, which is not desirable.

4. Implementation issues

In this section we discuss how to find the solution of the scheme (3.1), (3.10) and (3.3). Since the scheme is nonlinearly implicit we need to do a linearization and then solve a linear system at each time step. The model is non-symmetric, highly complex, and includes quite a number of parameters which may be large or small. It may not be robust and may not be easy to provide a theoretical justification of correct convergence when an iterative method is used to solve the resulting linear system. Hence, we solve the linear system using a direct method to avoid the uncertain performance of iterative methods and to ensure the correctness of the solution. On the other hand, looking at the scheme (3.1)–(3.3) with the Newton linearization the linear system depends on time. So we will have to solve a different linear system at every time step. This indicates that a direct method may be pretty costly. We thus look for an alternative linearization where the linear system may be symmetric but, more importantly, does not depend on time. Then we only need to have an LU or Cholesky kind of decomposition of the linear system at the beginning of time. After the initial time we do not need to solve any linear system when its coefficient matrix is time-independent. That is, we can compute the solution of the implicit scheme as if it is an explicit scheme.

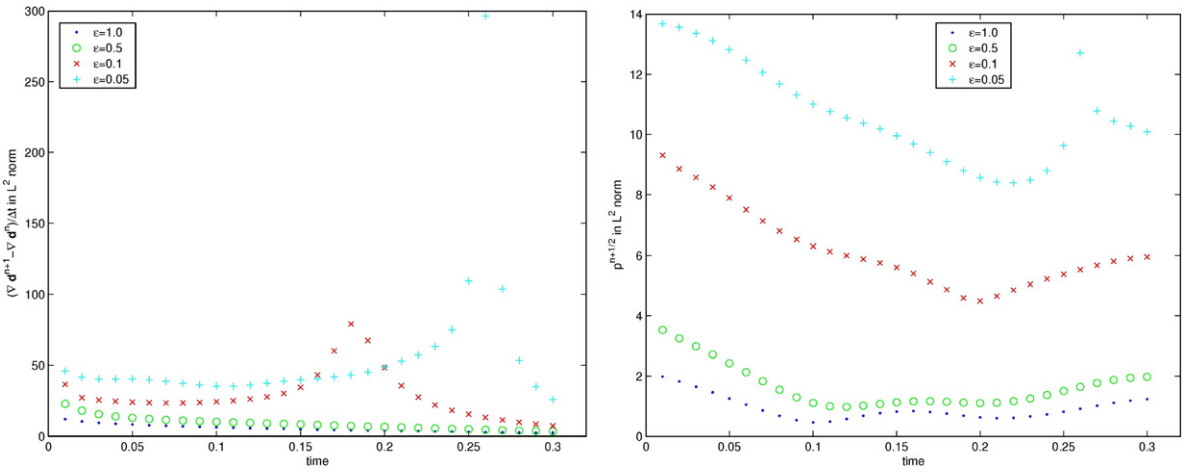

Fig. 1. $\|\mathbf{d}_t^{n+1}\|_{\mathbf{L}^2}$ and $\|p_h^{n+\frac{1}{2}}\|_{L^2}$ vs time for $\epsilon = 1.0, 0.5, 0.1$ and 0.05.

To achieve a time independent (or matrix free) linear system we propose to use a fixed point iteration as the linearization of all nonlinear terms. We thus have the following iterative scheme (for $s = 1, 2, \ldots$) at every time level t_n, i.e. find $\bar{\mathbf{u}}_s$, $\bar{p}_s$ and $\bar{\mathbf{d}}_s$ (as an approximation of $\mathbf{u}^{n+1}$, p^{n+1} and $\mathbf{d}^{n+1}$, respectively) to satisfy:

$$\begin{aligned}\int_\Omega \Bigg[& (\bar{\mathbf{u}}_s)_{\bar{t}} \cdot \mathbf{v} + \left(\frac{\mathbf{u}_h^n + \bar{\mathbf{u}}_{s-1}}{2} \cdot \nabla\right) \frac{\mathbf{u}_h^n + \bar{\mathbf{u}}_{s-1}}{2} \cdot \mathbf{v} + \frac{1}{2}\left(\nabla \cdot \frac{\mathbf{u}_h^n + \bar{\mathbf{u}}_{s-1}}{2}\right) \frac{\mathbf{u}_h^n + \bar{\mathbf{u}}_{s-1}}{2} \cdot \mathbf{v} + \nu \nabla \frac{\mathbf{u}_h^n + \bar{\mathbf{u}}_s}{2} : \nabla \mathbf{v} \\ & - \frac{p_h^n + \bar{p}_s}{2} (\nabla \cdot \mathbf{v}) + \frac{\lambda}{\gamma}\left((\bar{\mathbf{d}}_s)_{\bar{t}} + \left(\frac{\mathbf{u}_h^n + \bar{\mathbf{u}}_{s-1}}{2} \cdot \nabla\right) \frac{\mathbf{d}_h^n + \bar{\mathbf{d}}_{s-1}}{2} + D_\beta\left(\frac{\mathbf{u}_h^n + \bar{\mathbf{u}}_{s-1}}{2}\right) \frac{\mathbf{d}_h^n + \bar{\mathbf{d}}_{s-1}}{2}\right) \cdot (\mathbf{v} \cdot \nabla) \frac{\mathbf{d}_h^n + \bar{\mathbf{d}}_{s-1}}{2} \\ & + \frac{\lambda}{\gamma}\left((\bar{\mathbf{d}}_s)_{\bar{t}} + \left(\frac{\mathbf{u}_h^n + \bar{\mathbf{u}}_{s-1}}{2} \cdot \nabla\right) \frac{\mathbf{d}_h^n + \bar{\mathbf{d}}_{s-1}}{2} + D_\beta\left(\frac{\mathbf{u}_h^n + \bar{\mathbf{u}}_{s-1}}{2}\right) \frac{\mathbf{d}_h^n + \bar{\mathbf{d}}_{s-1}}{2}\right) \cdot D_\beta(\mathbf{v}) \frac{\mathbf{d}_h^n + \bar{\mathbf{d}}_{s-1}}{2}\Bigg] \mathrm{d}\mathbf{x} = 0,\end{aligned} \tag{4.1}$$

$$\int_\Omega \left(\nabla \cdot \frac{\mathbf{u}_h^n + \bar{\mathbf{u}}_s}{2} + \delta \frac{p_h^n + \bar{p}_s}{2}\right) q \, \mathrm{d}\mathbf{x} = 0, \tag{4.2}$$

$$\begin{aligned}\int_\Omega \Bigg[& (\bar{\mathbf{d}}_s)_{\bar{t}} \cdot \mathbf{e} + \left(\frac{\mathbf{u}_h^n + \bar{\mathbf{u}}_{s-1}}{2} \cdot \nabla\right) \frac{\mathbf{d}_h^n + \bar{\mathbf{d}}_{s-1}}{2} \cdot \mathbf{e} + D_\beta\left(\frac{\mathbf{u}_h^n + \bar{\mathbf{u}}_{s-1}}{2}\right) \frac{\mathbf{d}_h^n + \bar{\mathbf{d}}_{s-1}}{2} \cdot \mathbf{e} \\ & + \gamma \nabla \frac{\mathbf{d}_h^n + \bar{\mathbf{d}}_s}{2} : \nabla \mathbf{e} + \frac{\gamma}{\epsilon^2} \mathbf{g}_h(\mathbf{d}_h^n, \bar{\mathbf{d}}_{s-1}) \cdot \mathbf{e}\Bigg] \mathrm{d}\mathbf{x} = 0,\end{aligned} \tag{4.3}$$

where we can choose initial iteration as $\bar{\mathbf{u}}_0 = \mathbf{u}_h^n$ and $\bar{\mathbf{d}}_0 = \mathbf{d}_h^n$. We can easily see that the stiffness matrix at each time step is symmetric, independent of time and of the number of the fixed point iterations. From the discussion in [20] for the small molecule case the step size Δt has to satisfy $\gamma \Delta t < \epsilon^2$ to ensure that the fixed point method converges. This kind of restriction in Δt may be helpful from the accuracy point of view as well. However, for the model we are solving now, the condition is not enough for the convergence of the fixed point iteration (4.1)–(4.3). Even if we assume that the solution is sufficiently regular, when we conduct a convergence analysis of the method we will still have trouble, especially in dealing with the term $\frac{\lambda}{\gamma}(\bar{\mathbf{d}}_s)_{\bar{t}} \cdot D_\beta(\mathbf{v}) \frac{\mathbf{d}_h^n + \bar{\mathbf{d}}_{s-1}}{2}$ which does not appear in the small molecule case. Generally speaking, the convergence of the method may depend also on the ratio λ/γ as well as the solution due to the high nonlinearity. The smaller the ratio λ/γ is, the better the convergence of the fixed point method. Nevertheless, the method converges for all the numerical experiments given in the last section. We will provide an alternative treatment in Remark 4.1 if the fixed point method does not converge.

We would like to emphasize here that we want to use the fixed point iteration whenever possible not only because a symmetric stiffness matrix and a matrix free evolution process can be achieved but also because the system (4.1) and (4.2) for $\mathbf{u}$ and p and the system (4.3) for $\mathbf{d}$ are automatically separated. We can solve (4.3) first to obtain $\bar{\mathbf{d}}_s$, then solve (4.1) and (4.2) to get $\bar{\mathbf{u}}_s$ and $\bar{p}_s$. This further reduces the size of the system and the cost of computation.

Remark 4.1. If the fixed iterative method does not converge we may use the Newton's method. In this case we may not be able to pursue a matrix free evolution process. Due to high nonlinearity the Newton's iterative formulas may also be very complicated. An alternative is to use an explicit–implicit second order temporal discretization. That is, we approximate $\mathbf{u}_h^{n+1}$ and $\mathbf{d}_h^{n+1}$ in part of those nonlinear terms by $\mathbf{u}_h^n + \mathbf{u}_{\bar{t}}^n \Delta t = 2\mathbf{u}_h^n - \mathbf{u}_h^{n-1}$ and $\mathbf{d}_h^n + \mathbf{d}_{\bar{t}}^n \Delta t = 2\mathbf{d}_h^n - \mathbf{d}_h^{n-1}$, respectively. We thus have the following second order temporal scheme.

$$\begin{aligned}\int_\Omega \Bigg[& \mathbf{u}_{\bar{t}}^{n+1} \cdot \mathbf{v} + \left(\frac{3\mathbf{u}_h^n - \mathbf{u}_h^{n-1}}{2} \cdot \nabla\right) \mathbf{u}_h^{n+\frac{1}{2}} \cdot \mathbf{v} + \frac{1}{2}\left(\nabla \cdot \frac{3\mathbf{u}_h^n - \mathbf{u}_h^{n-1}}{2}\right) \mathbf{u}_h^{n+\frac{1}{2}} \cdot \mathbf{v} + \nu \nabla \mathbf{u}_h^{n+\frac{1}{2}} : \nabla \mathbf{v} - p_h^{n+\frac{1}{2}} (\nabla \cdot \mathbf{v}) \\ & + \frac{\lambda}{\gamma}\left(\mathbf{d}_{\bar{t}}^{n+1} + \left(\mathbf{u}_h^{n+\frac{1}{2}} \cdot \nabla\right) \frac{3\mathbf{d}_h^n - \mathbf{d}_h^{n-1}}{2} + D_\beta\left(\mathbf{u}_h^{n+\frac{1}{2}}\right) \frac{3\mathbf{d}_h^n - \mathbf{d}_h^{n-1}}{2}\right) \cdot (\mathbf{v} \cdot \nabla) \frac{3\mathbf{d}_h^n - \mathbf{d}_h^{n-1}}{2} \\ & + \frac{\lambda}{\gamma}\left(\mathbf{d}_{\bar{t}}^{n+1} + \left(\mathbf{u}_h^{n+\frac{1}{2}} \cdot \nabla\right) \frac{3\mathbf{d}_h^n - \mathbf{d}_h^{n-1}}{2} + D_\beta\left(\mathbf{u}_h^{n+\frac{1}{2}}\right) \frac{3\mathbf{d}_h^n - \mathbf{d}_h^{n-1}}{2}\right) \cdot D_\beta(\mathbf{v}) \frac{3\mathbf{d}_h^n - \mathbf{d}_h^{n-1}}{2}\Bigg] \mathrm{d}\mathbf{x} = 0,\end{aligned} \tag{4.4}$$

$$\int_\Omega \left[\left(\nabla\cdot\mathbf{u}_h^{n+\frac{1}{2}}\right)+\delta p_h^{n+\frac{1}{2}}\right]q\,\mathrm{d}\mathbf{x}=0, \tag{4.5}$$

$$\int_\Omega\left[\mathbf{d}_{\bar{t}}^{n+1}\cdot\mathbf{e}+\left(\mathbf{u}_h^{n+\frac{1}{2}}\cdot\nabla\right)\frac{3\mathbf{d}_h^n-\mathbf{d}_h^{n-1}}{2}\cdot\mathbf{e}+D_\beta\left(\mathbf{u}^{n+\frac{1}{2}}\right)\frac{3\mathbf{d}_h^n-\mathbf{d}_h^{n-1}}{2}\cdot\mathbf{e}+\gamma\nabla\mathbf{d}_h^{n+\frac{1}{2}}:\nabla\mathbf{e}+\frac{\gamma}{\epsilon^2}\mathbf{g}_h(\mathbf{d}_h^n,\mathbf{d}_h^{n+1})\cdot\mathbf{e}\right]\mathrm{d}\mathbf{x}=0, \tag{4.6}$$

where we take $\mathbf{g}_h$ to be the same as in (3.3). As shown in Remark 3.1 other choice of $\mathbf{g}_h$ may possibly cause inaccuracy in maintaining the discrete energy law. Similarly to the previous section, taking $\mathbf{v}=\mathbf{u}_h^{n+\frac{1}{2}}$, $q=p_h^{n+\frac{1}{2}}$ and $\mathbf{e}=\frac{\lambda}{\gamma}\mathbf{d}_{\bar{t}}^{n+1}$, we can easily derive a penalized discrete energy law:

$$\begin{aligned}\left(\frac{1}{2}\|\mathbf{u}_h^{n+1}\|_{\mathbf{L}^2}^2+\frac{\lambda}{2}\|\nabla\mathbf{d}_h^{n+1}\|_{\mathbf{L}^2}^2+\lambda\int_\Omega F(\mathbf{d}_h^{n+1})\right)_{\bar{t}}&=-\Big(v\|\nabla\mathbf{u}_h^{n+1}\|_{\mathbf{L}^2}^2+\delta\|p_h^{n+\frac{1}{2}}\|_{L^2}^2+\frac{\lambda}{\gamma}\|\mathbf{d}_{\bar{t}}^{n+1}\\&+(\mathbf{u}_h^{n+\frac{1}{2}}\cdot\nabla)\frac{3\mathbf{d}_h^n-\mathbf{d}_h^{n-1}}{2}+D_\beta(\mathbf{u}_h^{n+\frac{1}{2}})\frac{3\mathbf{d}_h^n-\mathbf{d}_h^{n-1}}{2}\|_{\mathbf{L}^2}^2\Big).\end{aligned} \tag{4.7}$$

In this scheme all equations are coupled to formulate a almost linear system with nonlinearity appeared only at $\mathbf{g}_h$ (thus simpler than (3.1)–(3.3). We may further simplify the scheme (if not deteriorating the stability) by replacing $\mathbf{u}_h^{n+\frac{1}{2}}$ and $\mathbf{d}_h^{n+\frac{1}{2}}$ in all trilinear terms by $\frac{3\mathbf{u}_h^n-\mathbf{u}_h^{n-1}}{2}$ and $\frac{3\mathbf{d}_h^n-\mathbf{d}_h^{n-1}}{2}$, respectively. Then we still have a second order temporal scheme and an $\mathrm{O}((\Delta t)^2)$ approximate energy law to (4.7) and at the same time make system (4.4),(4.5) and system (4.6) being separated, i.e. we can solve for $\mathbf{d}$ from (4.6) first and then solve for $\{\mathbf{u},p\}$ from (4.4),(4.5). The size of the system is thus significantly reduced. The nonlinear term $\mathbf{g}_h$ in system (4.6) may be dealt with by either the Newton's method or the fixed point method. If we use the fixed point method as before then we can have a matrix free iteration (i.e. the stiffness matrix is independent of the iteration) for the nonlinear system. Following the technique given in [20] we can also derive the convergence estimate:

$$\|\mathbf{d}_h^{n+1}-\bar{\mathbf{d}}_s\|_{\mathbf{L}^2}\leqslant\frac{\gamma M_d\Delta t}{\epsilon^2}\|\mathbf{d}_h^{n+1}-\bar{\mathbf{d}}_{s-1}\|_{\mathbf{L}^2},$$

where $M_d=\max_n||\mathbf{d}^n|^2-1|$. That is, for this simplified second order explicit–implicit scheme the fixed point nonlinear iteration converges if $\gamma M_d\Delta t/\epsilon^2<1$.

5. Numerical examples

In this section we would like to do a number of numerical experiments to demonstrate the proposed energy law preserving C^0 finite element method. We will also use the method developed in the paper to simulate kinematic effects through a few liquid crystal flow examples. The computations are carried out with the help of the freefem++ platform [4] and MATLAB.

We will consider the following singularity transportation example originally given in [21]. We will set the Reynolds number to be one. Some results for other Reynolds numbers will be given later. We apply the fixed point iterative method (cf. (4.1)–(4.3)) with a tolerance 10^{-5}.

Example 5.1. We consider the hydrodynamic liquid crystal model (1.1)–(1.3), where the initial director field $\mathbf{d}(\mathbf{x})=\tilde{\mathbf{d}}(\mathbf{x})/\sqrt{|\tilde{\mathbf{d}}(\mathbf{x})|^2+\epsilon^2}$, and

$$\tilde{\mathbf{d}}(\mathbf{x})=(x_1^2+x_2^2-\alpha^2,2\alpha x_2).$$

We simply choose $\alpha=0.5$. This director field has singularities at $\mathbf{x}=(\pm\alpha,0)$ with unit degrees of opposite signs. Let the initial flow field be zero. Two singularities would move towards the origin, meet and then disappear (annihilation). At the annihilation the energy will have a significant drop (see Fig. 6). So we roughly determine the annihilation time by observing that the energy starts to have a significant drop (for this example, it occurs when the energy drops below 10). We take $\epsilon^2=0.05^2$, $\Delta t=0.001$ and use a 16×16 grid in the computation.

From the computation we observe that the annihilation time is roughly $t = 0.262$ for this example using this energy law preserving method. The result is consistent when we use a smaller time step $\Delta t = 0.0001$ or use a finer mesh 64×64. This provides another evidence that the method is pretty robust in simulating the singularity transportation. We depict the director and flow fields at the annihilation time in Fig. 2. From the penalized divergence free Eq. (3.10) we have $\|\nabla \cdot \mathbf{u}_h^{n+\frac{1}{2}}\|_{L^2} \leqslant \delta \|p_h^{n+\frac{1}{2}}\|_{L^2}$. Fig. 1 indicates that $\max_n \|p_h^{n+\frac{1}{2}}\|_{L^2}$ is about 14, so $\|\nabla \cdot \mathbf{u}_h^{n+\frac{1}{2}}\|_{L^2} \leqslant 14\delta \approx 1.4 \times 10^{-5}$. So the divergence free condition is maintained well with the method. The following table gives roughly computed annihilation times for a number of values of β.

β	0.0	−0.2	−0.5	−0.8	−1.0
Annihilation time	0.267	0.262	0.251	0.238	0.231

The energy has no significant change after reaching 1.33249. We may consider the solution reaches the steady state at this energy. For different values of β the time when the solution reaches the steady state is slightly different (for example, $t = 0.73$ for $\beta = -1.0$, $t = 0.7$ for $\beta = -0.5$ and $t = 0.68$ for $\beta = 0.0$, respectively). But it seems that the steady state solution does not depend on β. Fig. 3 shows the steady state solution with $\beta = 0$, -0.5 and -1.0. We do not observe any significant difference between these figures with these different β values.

5.1. Computing the small molecule case with various Reynolds numbers

In [21,23,20] a simpler case where the liquid crystal molecule is assumed to be small is considered. Thus the motion of liquid crystal molecule is represented by the motion at its center of mass. The model is Eqs. (1.1)–(1.3) but removing $D_\beta(\mathbf{u})\mathbf{d}$ in (1.3) and removing its corresponding stress term (i.e. no last term in the left hand side of (1.1)). In [20] a weak form without replacing the stress term by (2.1) and (1.3) was adopted. Hence, the

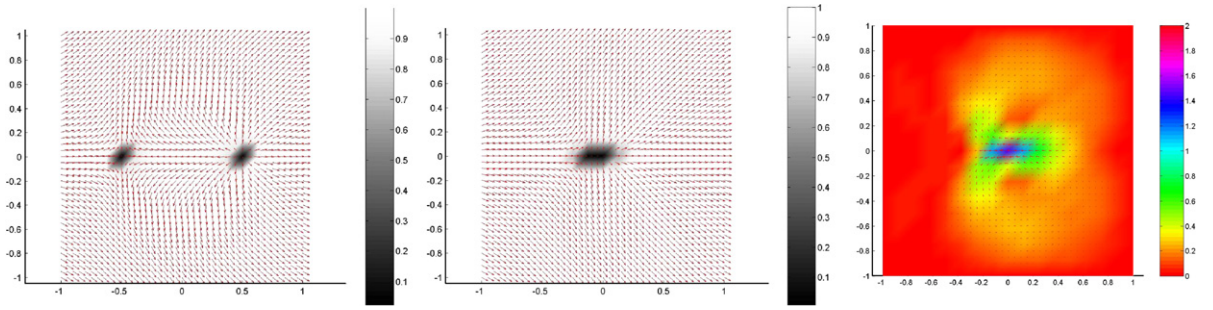

Fig. 2. Initial director field and director and flow fields at the annihilation time $t = 0.26$ with $\beta = -0.2$.

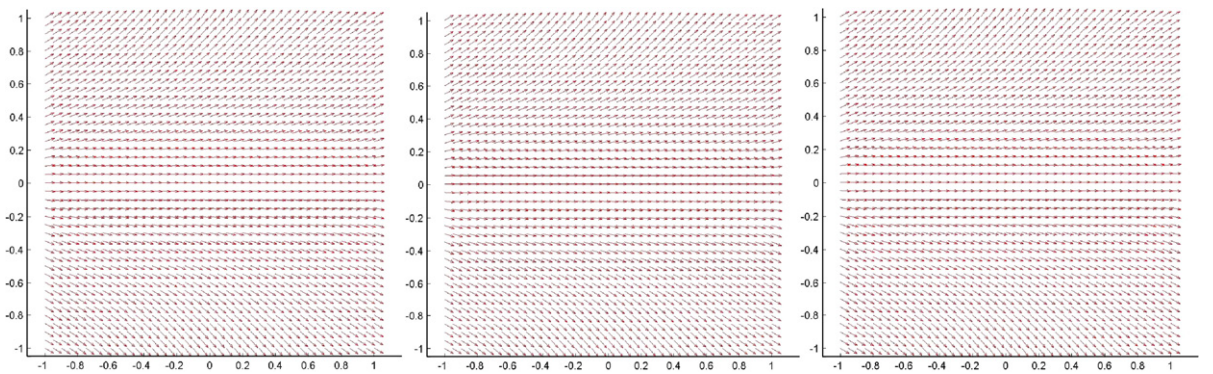

Fig. 3. The steady state director fields with $\beta = 0.0$, -0.5 and -1.0, respectively.

energy law cannot be rigorously derived if we do not assume the H^2 regularity of the solution of (1.3). It worked for the Example 5.1 and the annihilation time is given there for a few different Reynolds numbers.

In this section we would like to re-compute the small molecule model with those Reynolds numbers for the purpose of comparison. Since the annihilation time can only be given by observation it may not necessarily be accurate. So we will not compare the annihilation time but the time when the energy drops to certain level, for example, $E = 12.559$ (at $t = 0.26$ with $\mu = 1.0$ using the method proposed in [20]). We do six fixed point iterations in each time step and the iterative error is about 3×10^{-6}. The table below lists the time computed using the method (4.1)–(4.3) proposed in this paper for various Reynolds numbers or viscosity μ.

μ	1.0	0.1	0.01	0.001	0.0001
The time when $E \approx 12.559$	0.271	0.246	0.239	0.238	0.238

For $\mu = 1.0$ the time was $t = 0.26$ in [20] which is slightly different from $t = 0.271$ we obtained here. But the method used in [20] is based on a weak form without a rigorous continuous energy law. It does not have an accurate discrete energy law for the time-discretized system either. So we believe that the result we obtain here would be more reliable since the method is of second order in time and the energy law is accurately preserved if the fixed iterative method converges. Fig. 4 below depicts the director and flow fields at $t = 0.246$ for the case of $Re = 10$.

We also observed in [20] that near the annihilation time and in cases of the higher Reynolds number (i.e. $Re = 100$ and 1000) the velocity field near the singularity region looks messy or unclear and for $Re = 1000$ even a 64×64 grid was not enough and a much more refined grid around the singularity region was required. We believe that it is due to no rigorous continuous energy law in the direct weak form given in [20]. We thus re-compute the example for these two Reynolds numbers plus $Re = 10000$ using the weak form (2.2)–(2.4) we currently developed. Under this weak form the energy law has been rigorously derived and an accurate discrete energy law has been derived too. We observe that the velocity field can be well calculated even with a 16×16 grid. To see details of the velocity structure we will depict the result with a 64×64 grid. The director and velocity fields near its annihilation time (or when $E = 12.559$) are given in Fig. 5 for higher Reynolds numbers $Re = 100$, 1000 and 10000. We observe that under the energy-law preserving formulation presented in this paper the flow field $Re = 100$ and $Re = 1000$ is significantly more accurate near the center (where the singularity locates at the annihilation time) than those (Figs. 5 and 6) in [20]. In the case of $Re = 1000$ the method in [20] requires a finer mesh to achieve a reasonable results. This indicates that the energy law preserving formulation has a better stability as well.

Next figures we will see how the energy decays according to the viscosity or the Reynolds number ($\mu = 1,\ 0.1,\ 0.01$ and 0.001). In the computation we use a 16×16 grid and $\Delta t = 0.001$. We take $\epsilon^2 = 0.05^2$. We observe that a significant change of energy is accompanied with the annihilation.

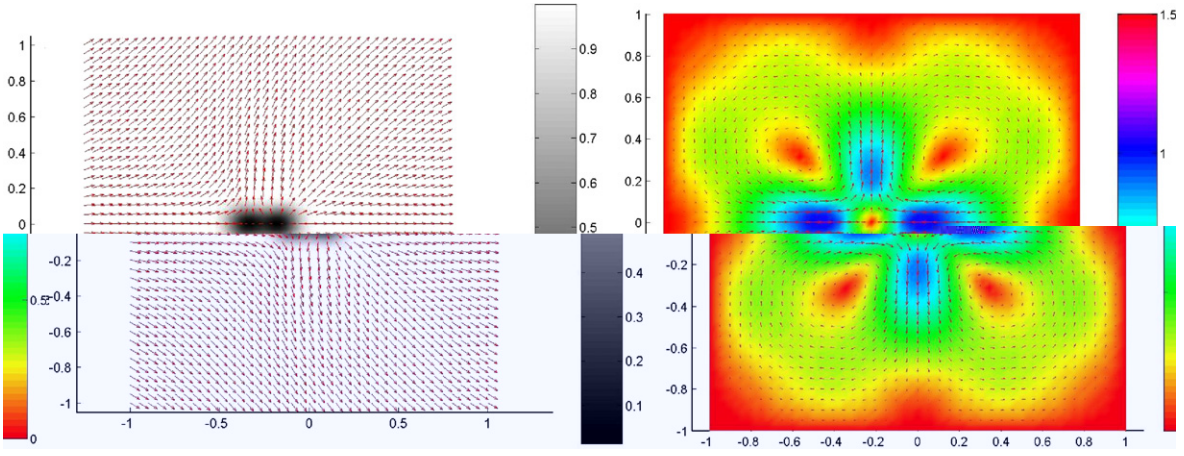

Fig. 4. Director and flow fields with $Re = 10$ near the annihilation time.

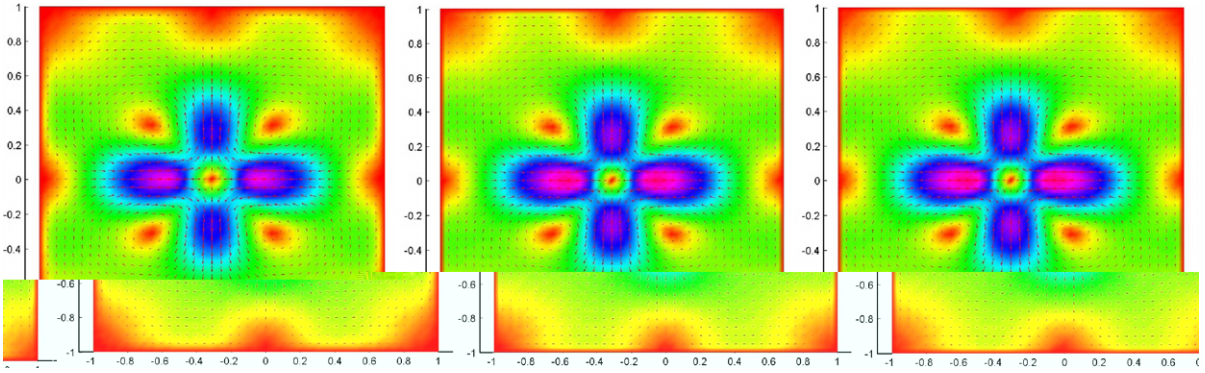

Fig. 5. Flow fields with $Re = 100$, 1000 and 10000 near the annihilation time.

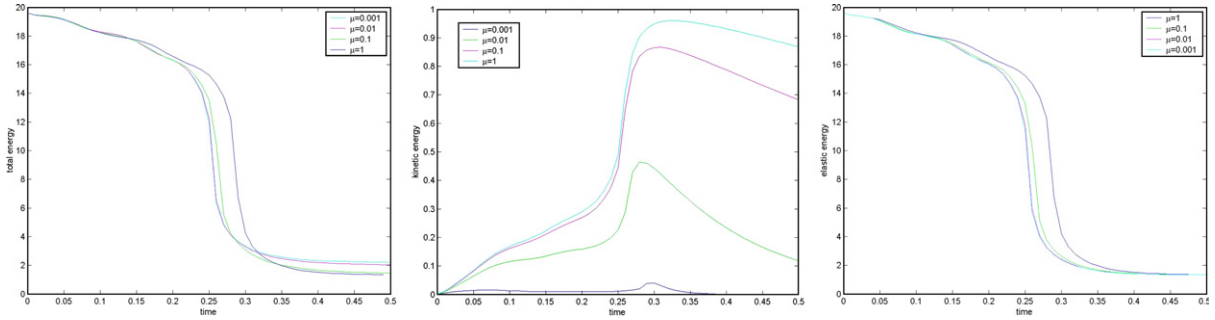

Fig. 6. Energy vs time.

5.2. Rheological behavior under different kinematic transportation

In this section we will consider the large molecule liquid crystal flow in a square domain or a square domain with a circular hole. Initial director field is the same as Example 5.1. Initial velocity field is either $\mathbf{u}_1 = (-\omega y, \omega x)$ or $\mathbf{u}_2 = (-\omega x, \omega y)$ (see Fig. 7). We would like to see how singularity transports in these velocity fields. Difference to the small molecule case (calculated in [20]) would be observed.

We first consider a square domain with a rotational velocity field $\mathbf{u}_1$ with $\omega = 20$. Fig. 8 depicted director fields at four different times. Clearly, the annihilation time is around $t = 0.2$.

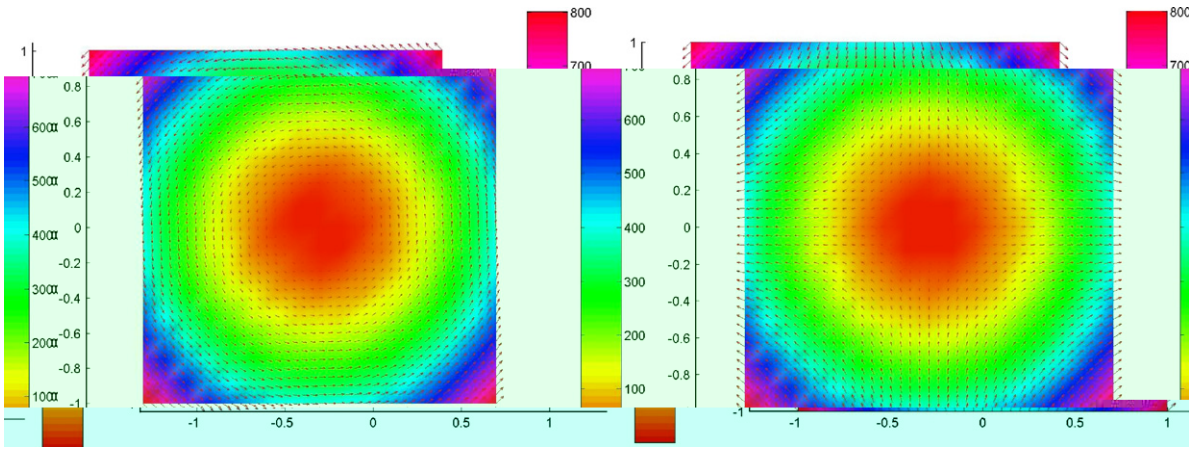

Fig. 7. Two types of rotational initial velocities $\mathbf{u}_1$ and $\mathbf{u}_2$ with $\omega = 20$.

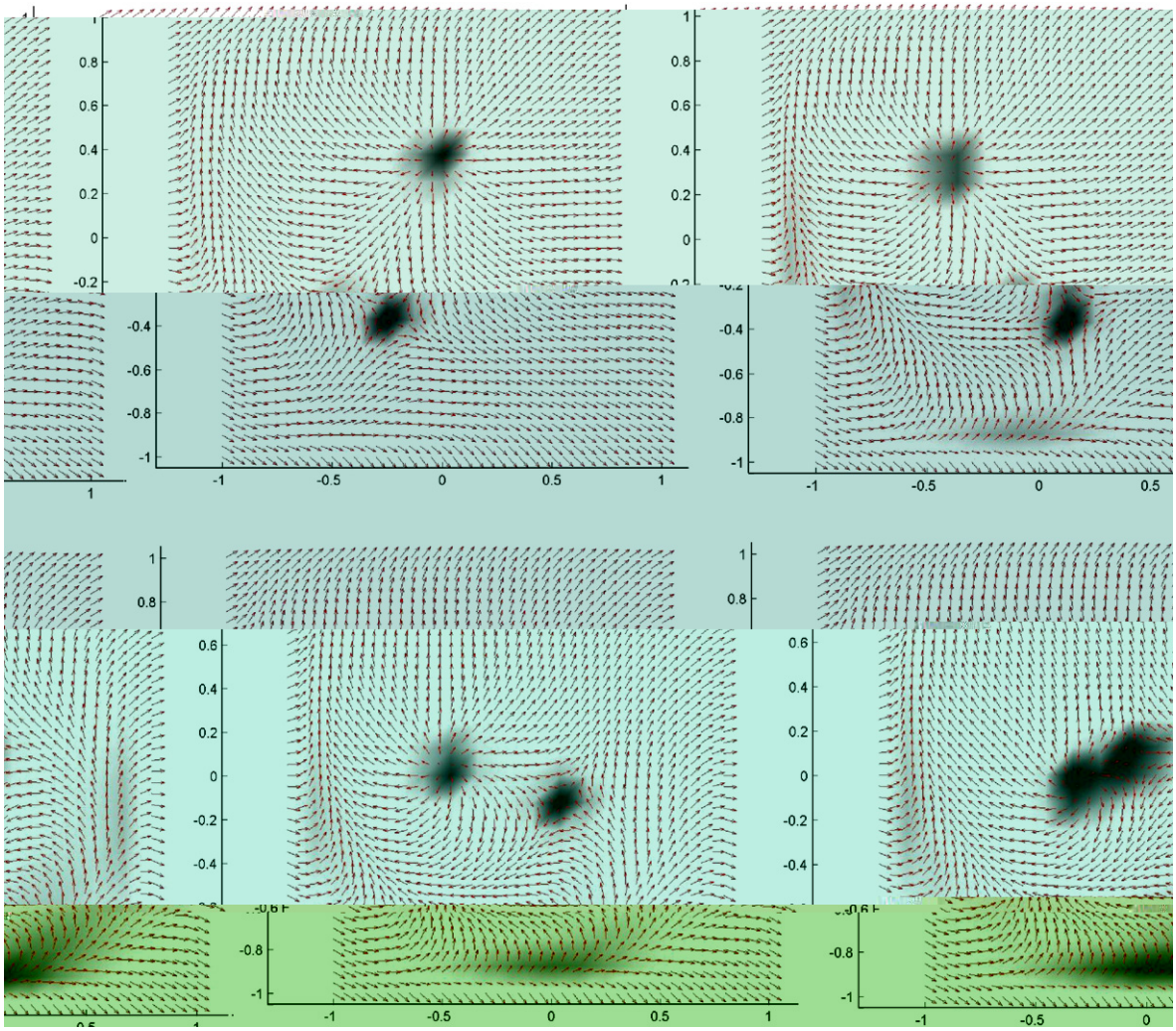

Fig. 8. Director fields at $t = 0.05$, 0.1, 0.15 and 0.2 in a square domain with the rotational velocity field $\mathbf{u}_1$ ($\omega = 20$).

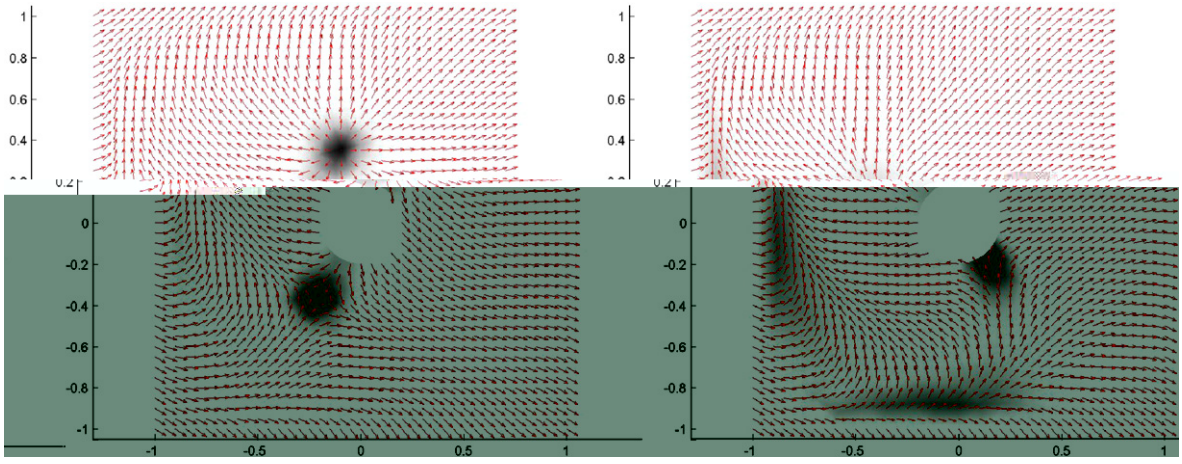

Fig. 9. Director fields at $t = 0.05$ and 0.1 in a square domain with a circular hole under the rotational velocity field $\mathbf{u}_1$ ($\omega = 20$).

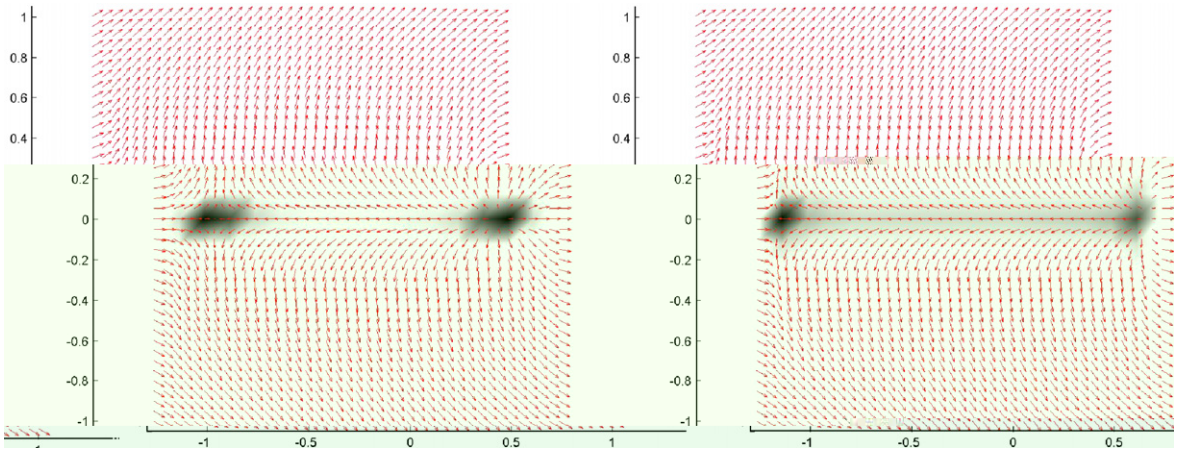

Fig. 10. Director fields at $t = 0.02$ and 0.04 in a square domain under the initial velocity field $\mathbf{u}_2$ ($\omega = 20$).

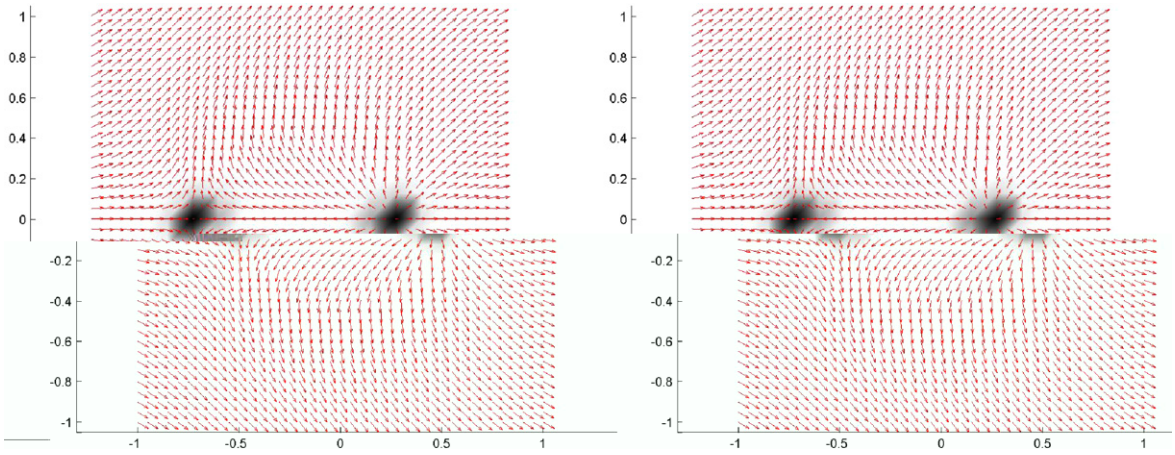

Fig. 11. Director fields at $t = 0.2$ and 0.4 in a square domain under the initial velocity field $\mathbf{u}_2$ ($\omega = 2$).

Next we calculate the same problem in a square domain with a circular hole. We have done the computation for small molecule model in [20] where two initial singularities approach the boundary of the circular hole and then rotate around the hole. These two singularities do not seem to annihilate in a pretty long time. But for the large molecule model we considered in this paper these two singularities annihilate roughly after $t = 0.2$. We also note difference of the molecule orientation pattern for small or large molecules are a bit different near the boundary. Fig. 9 shows the computational results.

If we consider another type of rotational velocity field $\mathbf{u}_2$. The flow field has direction opposite the moving direction of the singularity. If the flow velocity is fast (say, $\omega = 20$) two singularities will move along the flow direction and stop at the left and right sides of the square (see Fig. 10). If the flow velocity equals the velocity of the moving singularity (roughly, $\omega = 2$) we do not see that singularities move (see Fig. 11).

If the flow velocity is slower than $\omega = 2$ singularities will slowly move towards the center and annihilate at a much later time than that in the zero initial flow case.

Acknowledgments

This work was started when Lin was visiting Department of Mathematics of Penn State University in Spring 2006. His research is partially supported by Singapore academic research Grants R-146-000-053-112

and R-146-000-099-112. Liu is partially supported by NSF Grants DMS-0405850 and DMS-0509094. Zhang is partially supported by NSF of China 10401008 and state key basic research project of China 2005CB321704.

References

[1] R. Cohen, S.Y. Lin, M. Luskin, Relaxation and gradient methods for molecular orientation in liquid crystals, Comput. Phys. Commun. 53 (1989) 455–465.
[3] Q. Du, B.Y. Guo, J. Shen, Fourier spectral approximation to a dissipative system modeling the flow of liquid crystals, SIAM J. Numer. Anal. 39 (3) (2001) 735–762.
[4] F. Hecht, O. Pironneau, A. Le Hyaric, K. Ohtsuka, *FreeFem++* (Version 2.17-1), 2007 (http://www.freefem.org/ff++/ftp/freefem++doc.pdf).
[5] P.G. de Gennes, J. Prost, The Physics of Liquid Crystals, second ed., Oxford Science Publications, Oxford, 1993.
[7] J. Ericksen, Conservation laws for liquid crystals, Trans. Soc. Rheol. 5 (1961) 22–34.
[8] R. Glowinski, P. Lin, X.B. Pan, An operator-splitting method for a liquid crystal model, Comput. Phys. Commun. 152 (2003) 242–252.
[9] R. Glowinski, P. Le Tallec, Augmented Lagrangian and Operator-Splitting Methods in Nonlinear Mechanics, SIAM, 1989.
[11] G.B. Jeffery, The motion of ellipsoidal particles immersed in a viscous fluid, Roy. Soc. Lond. Proc. Ser. A 102 (1922) 161–179.
[12] N. Kuzuu, M. Doi, Constitutive equation for nematic liquid crystals under weak velocity gradient derived from a molecular kinetic equation, J. Phys. Soc. Jpn. 52 (10) (1983) 3486–3494.
[13] M. Lees, A priori estimates for the solutions of difference approximations to parabolic partial differential equations, Duke Math. J. 27 (1960) 297–311.
[15] F.H. Lin, C. Liu, Nonparabolic dissipative systems, modeling the flow of liquid crystals, Commun. Pure Appl. Math. 48 (1995) 501–537.
[16] F.H. Lin, C. Liu, Global existence of solutions for the Ericksen Leslie-system, Arch. Rat. Mech. Anal. 154 (2) (2001) 135–156.
[17] F.H. Lin, C. Liu, P. Zhang, On viscoelastic fluids, Commun. Pure Appl. Math. LVIII (2005) 1–35.
[18] P. Lin, A sequential regularization method for time-dependent incompressible Navier–Stokes equations, SIAM J. Numer. Anal. 34 (1997) 1051–1071.
[19] P. Lin, X.Q. Chen, M.T. Ong, Finite element methods based on a new formulation for the non-stationary incompressible Navier–Stokes equations, Int. J. Numer. Meth. Fluids 46 (2004) 1169–1180.
[20] P. Lin, C. Liu, Simulation of singularity dynamics in liquid crystal flows: a C^0 finite element approach, J. Comput. Phys. 215 (1) (2006) 348–362.
[21] C. Liu, Noel J. Walkington, Approximation of liquid crystal flows, SIAM J. Numer. Anal. 37 (3) (2000) 725–741.
[22] P. Lin, T. Richter, An adaptive homotopy multi-grid method for molecule orientations of high dimensional liquid crystals, J. Comput. Phys. 225 (2) (2007) 2069–2082.
[23] C. Liu, Noel J. Walkington, Mixed methods for the approximation of liquid crystal flows, M2AN 36 (2) (2002) 205–222.
[24] C. Liu, N.J. Walkington, An Eulerian description of fluids containing visco-hyperelastic particles, Arch. Ration. Mech. Anal. 159 (2001) 229–252.
[25] C. Liu, J. Shen, X. Yang. Dynamics of defect motion in nematic liquid crystal flow: modeling and numerical simulation, preprint, 2006.
[26] R. Temam, Navier–Stokes Equations, North-Holland, Amsterdam, 1977.